Assessment of a machine-vision-assisted test bed for spacecraft magnetic cleanliness analysis

Alejandro Sans Monguiló[1], *Bagus Adiwiluhung Riwanto*[2], *Jaan Praks*[2]

Abstract

Small satellites are becoming increasingly popular in several applications, in which attitude systems might require high precision performance. These spacecrafts are susceptible to magnetic disturbances in orbit, such as the interaction between the satellite and Earth's magnetic field. However, a major disturbance torque is generated by the residual magnetic moment. Therefore, a magnetic cleanliness analysis must be considered in order to meet the requirements for magnetic-sensitive instruments and subsystems. Studies on magnetic environment management are underway for the FORESAIL-1 and FORESAIL-2 missions using the optical magnetic test bed of Aalto University. This is particularly important for FORESAIL-2 which aims to precisely measure the orbital ambient magnetic field with a high sensitivity magnetometer

One of the parts of a spacecraft magnetic cleanliness analysis is the modelling of the residual magnetic moment as a set of magnetic dipoles. The dipoles are estimated from the measured magnetic field surrounded by the device-under-test (e.g., complete satellite, or its individual subsystems) using a stochastic estimation algorithm. The measurements are performed in a Helmholtz cage where the device and a low-noise magnetometer are placed, and detected by a smart camera using visual detection markers (ArUco). Information provided by the detection of the markers is then used for representing the position of the magnetometer and measured magnetic field points in the device-under-test coordinate frame.

The camera detection accuracy is improved with data fusion from several ArUco markers, and the system performance is assessed by verifying the estimated magnetic moment results using known permanent magnets. Using this methodology for calculating the residual magnetic moment, the system is able to estimate the dipole's position and magnetic vectors with a mean absolute error of 0.004 ± 9·10-7 m and 0.007 ± 1·10-4 A·m2 respectively. The test bed can be used for the characterization of the magnetic moment when measuring small satellites, or its components, in order to mitigate the residual magnetic moment.

Keywords

Magnetic dipole moment, Optical magnetic test bed, Residual magnetic moment, Small satellite, Spacecraft magnetic cleanliness analysis

[1] Aato University, Finland, alesansm@gmail.com
[2] Aalto University, Finland

Nomenclature

B	*Surrounding Magnetic Field*
B_r	*Residual Flux Density of the magnet*
m	*Dipole Moment (magnetic)*
m_{EXXX}	*Dipole Moment of Magnet EXXX*
T_m	*Magnetic Torque*
V_{EXXX}	*Volume of the magnet*
μ_0	*Magnetic Permeability*

Acronyms/Abbreviations

ADCS	*Attitude, Determination and Control Subsystem*
CC	*Closer Configuration*
DUT	*Device-under-test*
FC	*Further Configuration*
FOV	*Field Of View*
MDM	*Magnetic Dipole Moment*
MF	*Magnetic Field*
OMTB	*Optical Magnetic Test Bed*
PA	*Pointing Angle*
RMM	*Residual Magnetic Moment*
S/C	*Spacecraft*
VA	*View Area*

1. Introduction

As the number of applications for small satellites increases rapidly, the mission goals can be more demanding. For example, the attitude, determination and control subsystem (ADCS) can require precise pointing and orientation management to meet the mission objectives. ADCS can be composed out of sensors such as magnetometers, gyroscopes, among others. The sensor data will influence the operation of the actuators, such as magnetorquers, reaction wheels, etc.

Some of these components can be affected by magnetic disturbances, which is the residual magnetic moment (RMM) of the spacecraft (S/C), and which can be one of the main perturbances. In order to minimize this, a magnetic dipole moment (MDM) need to be characterized accordingly, so mitigation techniques can be considered [1].

The MDM can be determined with a wide range of methods. Most of them involve mechanical magnetic test bed in which the device-under-test (DUT) is rotated in one or more axis during the measurement. However, some studies in this field are using new technology by incorporating a visual system which can be denoted as optical magnetic test bed (OMTB) [2][3][4]. This paper presents the performance of the OMTB used in Aalto university for small satellites' MDM characterization.

2. Magnetic dipole measurement

2.1. Pose and optical recognition

In this paper, the orientation of an object is represented by the Euler angles which represent the attitude of an object based on three rotations on each of the axes: x, y, z, named pitch, yaw and roll respectively. The final rotated frame depends on the sequence of the rotations. Note that pose is defined as the position and the orientation combined.

The OMTB uses optical recognition to detect the pose of the DUT by using ArUco markers stuck on the faces of the device. These markers poses are defined in the detection algorithm and then gathered using a smart camera using machine vision [4]. The markers have different patterns which differentiate them from one another.

2.2. Magnetic torque and characterization

As it was stated earlier, the main perturbance comes from the residual S/C's dipole moment, also known as RMM. This magnetic torque can be expressed as

$$\mathrm{T_m} = m \times B \qquad (1)$$

In order to reduce the RMM of the S/C and mitigate its disturbance, it is important for magnetic characterization techniques to be able to model the MDM. So, it can be compensated such that only a RMM remains. Some of these techniques are presented in [2], which include: direct torque measurements, ambient field mapping, mapping in a field-free region, etc. The last technique requires a region where the ambient MF is nearly zero, so small size devices are normally measured using this technique.

This paper will focus on the last technique, where the different poses of the DUT are measured inside a field-free region. In mechanical magnetic test beds, the DUT is rotated using mechanical systems to gather the pose information. These systems can be complex, even making the measurement tedious. Using a OMTB though, the process of gathering the information needed is automated and it does not require complex mechanical systems for taking the measurement.

3. Permanent magnet verification

3.1. Magnetic measurements

The physical setup of the OMTB at Aalto University is composed of: a 3-axis Helmholtz coil cage, a magnetometer, the DUT, ArUco markers, camera and support, background isolation paper, and control software; as can be seen in Figure 1. The magnetometer is placed inside, at the center of the Helmholtz cage which generates a near-to-zero MF. The camera and the paper shall be placed in the near background, and stay in the same position throughout the measurement. The same applies to the computer. Then, the field-free region is generated inside the cage. Note that the DUT is placed when the measurement starts and is being rotated within the camera's field of view (FOV).

The visual from the camera is also available, where the orientation of the detected markers is displayed (Figure 2). The magnetometer has the marker '0', and the DUT is a cube of 50 mm x 50 mm x 50 mm where all faces are covered with markers from '1' to '6' of the size of 37.7 mm x 37.7 mm. The camera used is a Jevois-A33 smart video camera [5]. On the plane of the marker, the X-axis is horizontal towards the right, Y-axis is vertically upwards, and Z-axis follows the right-hand rule. Inside the DUT used, a permanent magnet is placed underneath marker '1' as shown in Figure 3. Note that its location shall be defined in the script [4].

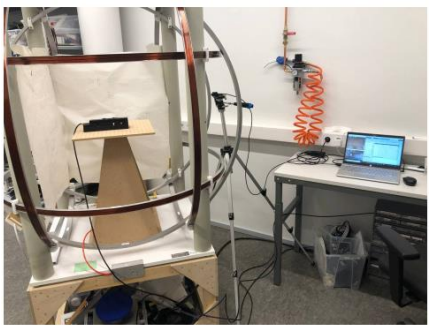

Figure 1. OMTB setup at Aalto University

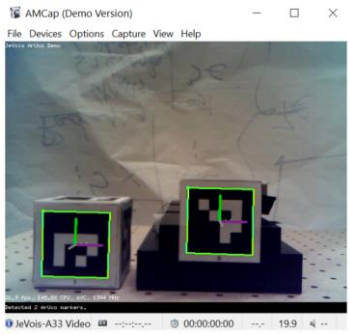

Figure 2. Marker detection from the camera

Figure 3. Permanent magnet E200's placement

Three magnets are evaluated. Their dipole moment can be calculated based on Eq. 2; where B_r is in Tesla, μ_0 in Henries per meter, and V_{EXXX} in cubic meters. The magnets are labeled with the codes E122, E317 and E200 (EXXX is generic). The characteristics of these magnets are displayed in Table 1. Note that the first magnet is cylindrical, and the rest are cubical.

For each of the magnets, the camera has been placed in a closer configuration (CC) and in a further configuration (FC), varying the distance from the markers and the camera. These two configurations can be seen in Figure 4 and Figure 1, respectively.

$$m_{EXXX} = \frac{B_r}{\mu_0} \cdot V_{EXXX} \qquad (2)$$

Table 1. Permanent magnets' features

Magnet label	Unit	E122	E317	E200
Radius	m	0.0017	-	-
Width		-	0.0050	0.0050
Depth		-	0.0050	0.0050
Height		0.0017	0.0020	0.0050
Position X-axis		0.0000	-0.0011	0.0000
Position Y-axis		0.0179	0.0180	0.0195
Position Z-axis		-0.0230	-0.0250	-0.0250
MDM X-axis	A·m2	0.0000	0.0000	0.0000
MDM Y-axis		±0.0039	±0.0509	±0.5093
MDM Z-axis		0.0000	0.0000	0.0000

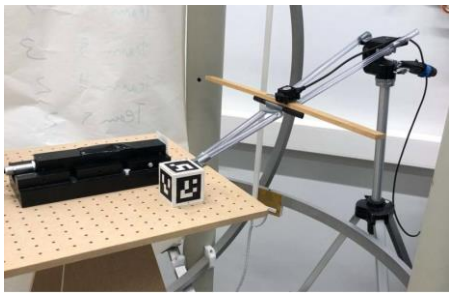

Figure 4. CC camera-marker

3.2. Modified magnetic measurements

some problems when detecting the markers were observed After taking the first round of measurements: momentarily undetected or intermittent marker detection, and orientation flipping. The way the software managed the collection of the marker's information was modified in order to minimize the effect of these problems. The next step was to analyze which poses provided improved accuracy. A better detection of the pose is proportionally related to a better reading and calculation of both position and MF. Thus, improving the detection of the markers' pose was the main focus, and a field-free region was not needed for this work.

For this evaluation, two markers were placed on a flat surface simulating one marker each for the magnetometer and one face of the DUT. Note that the markers do not move in relation to each other, the flat surface is rotating at different poses while the camera detects the markers. The position and orientation of the DUT marker '4' respect to the magnetometer marker '0' remains constant. Since markers' pose is well defined, the detected position and orientation directly provides the error; since the detection should match the defined value.

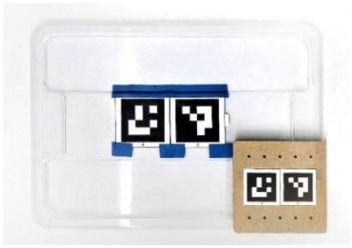

Figure 5. Markers '0' and '4' on a flat surface

It is worth to point out that several distances from the camera have been measured for different yaw and pitch angles of the flat surface. Roll angle has been proved not to disturb the detection when yaw and pitch angles are kept constant [5]. Notice that there are two sizes of markers, two markers for each flat surface. Markers are the same: '0' and '4' in both cases, but in different size: 37.7 mm x 37.7 mm, and 58 mm x 58 mm. Different size measurements have been considered to correlate the results in their detection's accuracy. The flat surfaces and the setup for this evaluation can be seen in Figure 5 and 6.

Figure 6. Accuracy evaluation set up

For analyzing the results, two generic concepts are created: pointing angle (PA) and view area (VA). PA refers to the axis angle of the DUT marker's Euler angles with respect to the camera z-axis pointing towards the markers, and VA is the percentage of marker's area viewed over the camera's FOV area. Based on this analysis, the algorithm has been modified to prioritize the detection of the markers in which pose the accuracy is higher. The three magnets and same camera configurations have been re-measured in order to see the new performance of the OMTB.

4. Results

The results from the first six measurements are displayed in Table 2, 3 and 4. Followed by the accuracy detection map based on the PAs and VAs, and their detection errors in position and orientation (Figure 7 and 8). Lastly, Table 5, 6 and 7 present the results of the modified magnetic measurements using the same magnets and configurations.

Table 2. Actual, CC and FC results

Magnet E122	Unit	Actual	CC	FC
Position X-axis	m	0.0000	0.0012	-0.0018
Position Y-axis		0.0179	0.0186	0.0143
Position Z-axis		-0.0230	-0.0237	-0.0256
MDM X-axis	A·m2	0.0000	-0.0006	0.0004
MDM Y-axis		±0.0039	-0.0061	-0.0045
MDM Z-axis		0.0000	0.0002	0.0002
MDM Module		0.0039	0.0062	0.0045

Table 3. Actual, CC and FC results

Magnet E317	Unit	Actual	CC	FC
Position X-axis	m	-0.0011	-0.0023	0.0007
Position Y-axis		0.0180	0.0205	0.0176
Position Z-axis		-0.0250	-0.0259	-0.0241
MDM X-axis	A·m2	0.0000	0.0013	0.0039
MDM Y-axis		±0.0509	-0.0469	-0.0345
MDM Z-axis		0.0000	-0.0002	-0.0013
MDM Module		0.0509	0.0469	0.0350

Table 4. Actual, CC and FC results

Magnet E200	Unit	Actual	CC	FC
Position X-axis	m	0.0000	0.0041	0.0000
Position Y-axis		0.0195	0.0152	0.0211
Position Z-axis		-0.0250	-0.0263	-0.0269
MDM X-axis	A·m2	0.0000	0.0627	0.0019
MDM Y-axis		±0.5093	0.3986	-0.4564
MDM Z-axis		0.0000	-0.0210	0.0064
MDM Module		0.5093	0.4041	0.4565

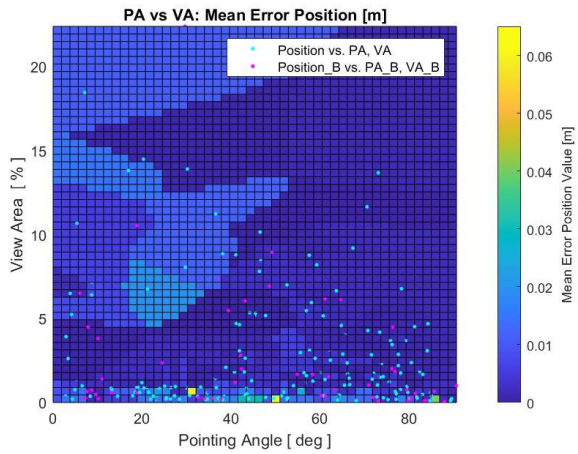

Figure 7. VA vs PA, mean error in position

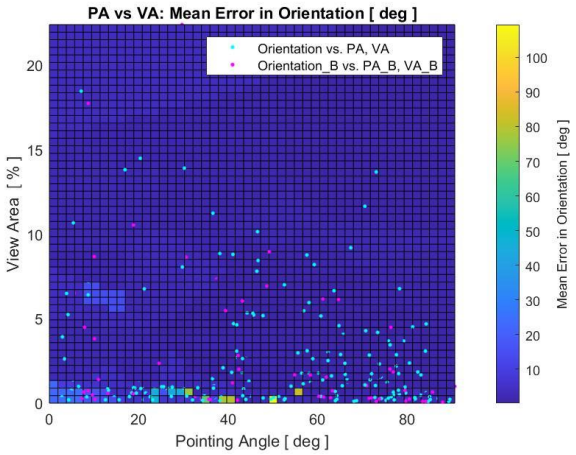

Figure 8. VA vs PA, mean error in orientation

Table 5. Actual, CC and FC after modification

Magnet E122	Unit	Actual	CC	FC
Position X-axis	m	0.0000	0.0017	0.0000
Position Y-axis		0.0179	0.0195	0.0090
Position Z-axis		-0.0230	-0.0239	-0.0257
MDM X-axis	A·m2	0.0000	-0.0005	0.0005
MDM Y-axis		±0.0039	-0.0061	-0.0033
MDM Z-axis		0.0000	0.0003	-0.0004
MDM Module		0.0039	0.0061	0.0034

Table 6. Actual, CC and FC after modification

Magnet E317	Unit	Actual	CC	FC
Position X-axis	m	-0.0011	0.0009	-0.0027
Position Y-axis		0.0180	0.0200	0.0175
Position Z-axis		-0.0250	-0.0245	-0.0225
MDM X-axis	A·m2	0.0000	0.0012	0.0011
MDM Y-axis		±0.0509	-0.0499	-0.0420
MDM Z-axis		0.0000	-0.0005	-0.0036
MDM Module		0.0509	0.0500	0.0422

Table 7. Actual, CC and FC after modification

Magnet E200	Unit	Actual	CC	FC
Position X-axis	m	0.0000	-0.0018	-0.0008
Position Y-axis		0.0195	0.0219	0.0182
Position Z-axis		-0.0250	-0.0282	-0.0334
MDM X-axis	A·m2	0.0000	0.0079	0.0162
MDM Y-axis		±0.5093	0.4258	-0.3872
MDM Z-axis		0.0000	-0.0103	-0.0126
MDM Module		0.5093	0.4041	0.4260

5. Discussion

From the first round of measurements, it can be said that the estimation in both configurations is similar.

The problems in the detection were observed and minimized by using the modified script based on the accuracy evaluation. In this evaluation, it can be seen that the detected orientation is homogeneously accurate at different distances from the camera but detection struggles around a PA of 40 degrees. Regarding the detection of the position, the accuracy is higher when the marker is oriented at a PA greater than 45 degrees; the accuracy also seems to vary with distance, but not by a significant amount. Comparing the modified magnetic measurements to the first round of measurements, there is a 2% increase in accuracy in the overall estimation results.

Based on these measurements and analysis, the OMTB is able to estimate the MDM's position and properties with a mean absolute error of 0.004 ± 9·10-7 m and 0.007 ± 1·10-4 A·m2, respectively. Moreover, it can be stated that the OMTB has an overall percentage error of 13% for position and 23% for magnetic properties, in the MDM estimation results.

More detailed information about the methodology, evaluation of the accuracy and measurements can be found mainly in [5]; regarding the particle swarm algorithm used to model the MDM, see [4].

6. Conclusions

The OMTB at Aalto University is able to model and estimate the MDM properties of the three permanent magnets used. The system was successfully assessed by measuring different magnetic dipoles before and after an evaluation and improvement of the accuracy in the markers' pose detection.

Future measurements could involve components of small satellites, or the spacecrafts themselves, in order to adjust and reduce the RMM. Also, the possibility of improving the results by carrying out improvements to the smart camera, lighting conditions, location of the OMTB and automatization of the DUT's rotation.

Acknowledgements

I would like to thank Jaan Praks and Bagus A. Riwanto for their help and guidance throughout the project. Also, to Daniel Garcia-Almiñana for the support for participating at the SSEA 2022.

Note that the participation in this conference (SSEA 2022) has received funding from the European Union's Horizon 2020 research and innovation programme under grant agreement No 737183. This reflects only the author's view and the European Commission is not responsible for any use that may be made of the information it contains.

References

[1] A. Lassakeur, C. Underwood, B. Taylor, and R. Duke, Magnetic cleanliness program on CubeSats and nanosatellites for improved attitude stability. *Journal of Aeronautics and Space Technologies*, 17, 2020.

[2] S. Schalkowsky, M. Harris, Spacecraft magnetic torques (Guidance and Control), NASA, 1969.

[3] D. Modenini, A. Bahu, G. Curzi, A. Togni, A dynamic testbed for nanosatellites attitude verification, *Aerospace,* 19, 2020.

[4] B. A. Riwanto, Calibration and testing techniques for nanosatellites attitude system development in magnetic environment, Doctoral thesis, Aalto University, 2021.

[5] A. Sans Monguiló, Magnetic moment characterization for small satellites, Master's thesis, Aalto University, 2021.